Cytochrome P450 3A Conjugation to Ubiquitin in a Process Distinct from Classical Ubiquitination Pathway

R. C. ZANGAR, A. L. KIMZEY, J. R. OKITA, D. S. WUNSCHEL, R. J. EDWARDS, H. KIM, and R. T. OKITA

Pacific Northwest National Laboratory, Richland, Washington (R.C.Z., A.L.K., D.S.W.); Washington State University, Pullman, Washington (J.R.O., R.T.O.); Faculty of Medicine, Imperial College, Hammersmith Campus, London, England (R.J.E.); and Detroit R&D, Inc, Detroit, Michigan (H.K.)

This article is available online at http://molpharm.aspetjournals.org

ABSTRACT

We characterize a novel microsome system that forms high-molecular-mass (HMM) CYP3A, CYP2E1, and ubiquitin conjugates, but does not alter CYP4A or most other microsomal proteins. The formation of the HMM bands was observed in hepatic microsomes isolated from rats treated 1 week or more with high doses (50 mg/kg/day) of nicardipine, clotrimazole, or pregnenolone 16α-carbonitrile, but not microsomes from control, dexamethasone-, nifedipine-, or diltiazem-treated rats. Extensive washing of the microsomes to remove loosely attached proteins or cytosolic contaminants did not prevent the conjugation reaction. In contrast to prototypical ubiquitination pathways, this reaction did not require addition of ubiquitin, ATP, Mg^{2+}, or cytosol. Addition of cytosol did result in the degradation of the HMM CYP3A bands in a process that was not blocked by proteasome inhibitors. Immunoprecipitated CYP3A contained HMM ubiquitin. Even so, mass spectrometric analysis of tryptic peptides indicated that the HMM CYP3A was in molar excess to ubiquitin, suggesting that the formation of the HMM CYP3A may have resulted from conjugation to itself or a diffuse pool of ubiquitinated proteins already present in the microsomes. Addition of CYP3A substrates inhibited the formation of the HMM CYP3A and the cytosol-dependent degradation of HMM CYP3A. These results suggest that after extended periods of elevated CYP3A expression, microsomal factors are induced that catalyze the formation of HMM CYP3A conjugates that contain ubiquitin. This conjugation reaction, however, seems to be distinct from the classical ubiquitination pathway but may be related to the substrate-dependent stabilization of CYP3A observed in vivo.

Cytochromes P450 (P450) constitute a superfamily of cysteine thiolate enzymes that catalyze a diverse array of biochemical reactions (Nelson et al., 1996). CYP3A is a subfamily of integral membrane proteins that are expressed at high levels in the endoplasmic reticulum (ER) of liver and intestine. In humans, CYP3A is important in the metabolism of approximately 50% of all prescribed drugs as well as lipophilic hormones such as testosterone (Guengerich, 1999). As a result of this broad substrate specificity and high level of expression, drug-drug interactions resulting from altered CYP3A activity are well documented (Thummel and Wilkinson, 1998).

After heme destruction and denaturation by reactive metabolites, CYP3A and CYP2E1 have been reported to be degraded by the ubiquitin-proteasome system (Correia et al., 1992; Tierney et al., 1992). Even in the absence of denaturation by reactive metabolites, these two P450s have relatively short half-lives (~7–10 h) compared with most other P450s or resident ER proteins (typical $t_{1/2}$ of 18–36 h) (Watkins et al., 1987; Koop and Tierney, 1990). Polyubiquitination commonly marks a protein for degradation by the 26S proteasome (Brodsky and McCracken, 1999; Schwartz and Ciechanover, 1999). Covalent linkage of ubiquitin typically requires the sequential action of a three-enzyme system. The first enzyme, ubiquitin-activating enzyme or E1, conjugates the ubiquitin C-terminal Gly to a Cys on the E1 enzyme. This thiolester-forming reaction is dependent upon ATP hydrolysis and Mg^{2+}. The ubiquitin C-terminal glycine is then transferred to a ubiquitin carrier protein (E2). Transfer of the ubiquitin to a protein substrate typically requires recognition of the protein substrate by a ubiquitin protein ligase (E3). Addition of subsequent ubiquitins to a monoubiquitinated protein commonly proceeds on the initial ubiquitin side chain rather than on another Lys in the substrate protein. Methylated ubiquitin (MeUb), in which the lysines are blocked but the reactive C-terminal glycine is intact, will inhibit polyubiquitination reactions after one or a few MeUb molecules are attached to the substrate protein. Although it has not

ABBREVIATIONS: P450, cytochrome P450; ER, endoplasmic reticulum; MeUb, methylated ubiquitin; HMM, high molecular weight; PAGE, polyacrylamide gel electrophoresis; IEF, isoelectric focusing; 2D, two dimensional; DMSO, dimethyl sulfoxide; CHAPS, 3-[(3-cholamidopropyl)dimethylammonio]propanesulfonate; MS, mass spectrometry; MS/MS, tandem mass spectrometry; PXR, pregnane X receptor.

been shown whether the ubiquitin/proteasome system contributes to the relatively short half-life of these P450s, it is interesting that both CYP3A and CYP2E1 generate high levels of reactive oxygen species and that this NADPH-dependent oxidase activity is inhibited by the presence of P450 substrate (Persson et al., 1990; Puntarulo and Cederbaum, 1998). The presence of substrate also stabilizes these P450s such that their half-lives are comparable with other ER proteins (Watkins et al., 1987). As such, it has been postulated that generation of reactive oxygen species by CYP3A and CYP2E1 may result in heme modification and subsequent protein degradation by the ubiquitin/proteasome system in a manner analogous to inactivation by reactive metabolites (Korsmeyer et al., 1999).

In this study, we demonstrated that hepatic microsomes from nicardipine-treated rats generate HMM CYP3A that is complexed with polyubiquitin. Similar to in vivo, CYP3A substrates blocked the formation of the HMM CYP3A bands. The formation of the HMM CYP3A bands was independent of the addition of ATP, Mg^{2+}, or cytosol and therefore was distinct from the classical E1-dependent ubiquitination process. Although addition of cytosol resulted in the loss of the HMM CYP3A, proteasome inhibitors did not affect this degradative process. Furthermore, peptide fingerprinting analysis of the HMM bands strongly suggested that CYP3A proteins were present in molar excess relative to ubiquitin conjugates, consistent with the concept that the shift of CYP3A into the HMM region was not simply the result of addition of a chain of ubiquitin molecules. Combined, these data suggest an alternative pathway for CYP3A degradation other than the classical ubiquitin/proteasome pathway and that this pathway may be important in the substrate-mediated stabilization of CYP3A.

Experimental Procedures

Materials. Powdered rat chow was purchased from Harlan Teklad (Madison, WI). CYP2E1 antibody was purchased from Oxygene (Dallas, TX). Anti-peptide antibodies specific for CYP3A2 and CYP3A23 have been described previously (Debri et al., 1995; Zangar et al., 1999). Polyclonal antibodies against rat CYP4A or CYP3A were purchased from Gentest (Woburn, MA). A monoclonal antibody raised against ubiquitin was obtained from Santa Cruz Biotechnology (Santa Cruz, CA). An antibody raised against an N-terminal peptide of the ubiquitin-activating enzyme E1 was obtained from Calbiochem (San Diego, CA). Secondary antibodies, conjugated to horseradish peroxidase, were obtained from Jackson Immunoresearch Laboratories, Inc. (West Grove, PA). SuperSignal West Pico chemiluminescent reagent, GelCode Blue protein stain, and bisacrylamide/azolactone "Ultralink" beads were obtained from Pierce Chemical (Rockford, IL). Novex 4 to 20% SDS-PAGE minigels were from Invitrogen (Carlsbad, CA). MeUb was from Affiniti Research Products (Mamhead, UK). Lactacystin, MG132, and protease inhibitor I were from Calbiochem. Isoelectric focusing (IEF) strips, Immobilized pH gradient buffer, urea, thiourea, and dithiothreitol used for two-dimensional (2D) gels were from Amersham Biosciences, Inc. (Piscataway, NJ). The Plus-One silver staining kit and Nonidet P-40 were from Amersham Biosciences, Inc. Micro Bio-Spin columns were from Bio-Rad (Hercules, CA). Centricon C-10s were from Amicon (Beverly, MA). Other reagents, including the polyclonal ubiquitin antibody and the calcium channel antagonists were from Sigma Chemical (St. Louis, MO).

Animals. Six-week-old male Sprague-Dawley rats (Simonsen Labs, Gilroy, CA) were used in all studies. Nicardipine, nifedipine, diltiazem, clotrimazole, and pregnenolone 16α-carbonitrile were typically mixed with unsweetened applesauce and the mixture was then added to powdered rat chow. Control rats were also fed the same powdered rat chow diet containing applesauce, but without the drugs. In one study, nicardipine (100 mg/kg/day) was diluted in 0.5% methylcellulose (1 ml/kg) and administered by gavage for 1, 2, or 3 days before sacrifice. For this study, control animals were gavaged with 0.5% methylcellulose alone. Food was removed from the rats 12 to 15 h before they were sacrificed. Induction of CYP3A by dexamethasone was undertaken using the treatment regimen described previously (Sherratt et al., 1989). This regimen calls for treating rats with intraperitoneal injections of 10 mg of dexamethasone/kg/day for 4 days and then sacrificing 24 h after the last treatment. In all studies, rats were sacrificed by administering sodium pentobarbital to induce anesthesia before removal of the livers. Microsomes and cytosols were prepared as described previously (Okita et al., 1993). Protein concentrations were determined as described previously (Lowry et al., 1951). Microsome aliquots were stored at $-80°C$ for 1 year or more without previous thawing and refreezing.

Primary Cultured Rat Hepatocytes. Primary cultures of rat hepatocytes were isolated and cultured as described previously (Zangar et al., 1995). Cells were cultured without treatment for 3 days before the initiation of a 30-h treatment with 2 mM phenobarbital or 10 μM dexamethasone. The last 6 h of treatment with these CYP3A-inducing drugs, cells were cotreated with 10 μM cycloheximide with or without 330 μM nicardipine or 0.1% DMSO (v/v).

Western Blots. Western blots were prepared as described previously (Zangar et al., 1993). Protein bands were imaged and quantitated by chemiluminescence with a Lumi-Imager F1 (Roche Applied Science, Indianapolis, IN). Two ubiquitin antibodies were used, a polyclonal and a monoclonal antibody, to ensure that the HMM ubiquitin banding pattern was reproducible with different antibodies. These ubiquitin antibodies gave essentially identical results in side-by-side comparisons and were used interchangeably in these studies. Primary antibodies were diluted as follows: anti-CYP3A23, 1:40,000; anti-CYP3A2, 1:100,000; anti-CYP2E1, 1:60,000; anti-CYP4A, 1:60,000; polyclonal anti-ubiquitin, 1:200; monoclonal anti-ubiquitin, 1:750; and anti-E1 ubiquitin-activating enzyme, 1:2000. Secondary antibodies were used at 1:5000 dilutions.

Microsome Incubation Reactions. Incubations were undertaken at 37°C using 75 μg of microsomal protein, 50 mM Tris, pH 7.5, 25 mM sucrose, 0.154 mM KCl, 2 mM $CaCl_2$, 3 μM $ZnCl_2$, 5 mM Na_2ATP, and 1 μM ubiquitin in a total volume of 50 μl unless noted otherwise. Reactions were terminated by addition of 50 μl of SDS-PAGE loading buffer (62.5 mM Tris, pH 6.8, 1% SDS, 11% glycerol, 370 μM bromphenol blue, and 0.5% 2-mercaptoethanol) and heating to 98°C for 5 min. To examine cytosol-dependent proteolysis, cytosol was added to the microsome incubates in some cases. In such cases, the amount of each reagent added to the incubation solution was adjusted to maintain the same concentration in the final reaction volume of 50 μl. After completion of the incubation, the microsomes were pelleted by ultracentrifugation before analysis by Western blotting.

To determine whether the cytosolic protein contamination may be important in the formation of HMM CYP3A bands, microsomes were incubated under conditions known to remove loosely bound proteins (Ploegh, 1997; von Wachenfeldt et al., 1997; Hori et al., 1999; Cosme and Johnson, 2000). These conditions included high salt (1 M NaCl, 10 mM KPO_4, 20% glycerol, 0.5 mM EDTA, and 10 mM 2-mercaptoethanol), low salt (10 mM KPO_4, 20% glycerol, 0.5 mM EDTA, and 10 mM 2-mercaptoethanol), high pH (0.1 M $NaCO_3$, pH 11.5, 6 mM sucrose, and 0.2 mM Tris, pH 7.5), mild detergent (0.017% deoxycholate, 13 mM Tris, pH 7.5, 33 mM KCl, 17 M sucrose, and 7 mM 2-mercaptoethanol), or the reaction buffer as a control (50 mM Tris, pH 7.5, 25 mM sucrose, and 150 mM KCl). Microsomes were diluted in each of these solutions, incubated on ice for 1 h, and centrifuged at 100,000g for 30 min. The microsomal pellet was resuspended and assayed for CYP3A-conjugating activity as described above.

Two-Dimensional Gels. Microsomal samples were incubated as described above except that the reaction was scaled up to 800 μl. To decrease salts that interfere with the IEF step, after incubation the microsomes were pelleted by ultracentrifugation and resuspended in 25 mM Tris, pH 7.5, 12.5 mM sucrose, 75 mM KCl. IEF strips, pH 4 to 7, were rehydrated overnight in a solution containing 7 M urea, 2 M thiourea, 4% CHAPS, 2% IEF buffer, pH 4 to 7, 65 mM dithiothreitol, 1 mM Tris, pH 7.5, 0.5 mM sucrose, 3 mM KCl, 0.01% bromphenol blue, and 125 μg of microsomal protein. IEF was carried out by linearly increasing from 0 to 500 V over the first 0.1 h, continuing at 500 V for 1 h, and then linearly increasing to 3500 V over 5 h and maintaining at 3500 V for 12 h. After focusing, the strips were incubated first in 2% lauryl sulfate, 50 mM Tris, pH 8.8, 6 M urea, 30% glycerol, 0.01% bromphenol blue, and 65 mM dithiothreitol for 1 h, and then for 15 min in the same solution except that the dithiothreitol was replaced with 135 mM iodoacetamide. The strips were then placed on top of an 8% SDS-PAGE gels and the gels were run as described previously (Zangar et al., 1993). The gels were silver stained with the Plus One kit (Amersham Biosciences, Inc.), according to the manufacturer's instructions.

Peptide Fingerprinting and MS/MS Analyses. Microsomes from rats treated with 100 mg of nicardipine/kg/day were incubated as described above. Samples were denatured in SDS-PAGE loading buffer (63 mM Tris, pH 6.8, 1% SDS, 1.5 M glycerol, 370 μM bromphenol blue) by heating to 65°C for 5 min. Denatured samples were loaded onto a 4 to 20% acrylamide gel and electrophoresed for 1 h at 20 mA. Gels were rinsed in deionized water three times for 5 m each, stained in GelCode Blue for 1 h, and washed with water for 1 h. Protein bands were excised with a sterile scalpel, transferred to a 500-μl microcentrifuge tube, and crushed. To destain the protein, 400 μl of acetonitrile/25 mM aqueous ammonium bicarbonate (1:1, v/v) was added, the tubes were vortexed and then allowed to sit for 10 min. The liquid was removed using a gel-loading pipette tip. This destaining step was repeated once. The gel was dehydrated by addition of 400 μl of acetonitrile, quickly vortexed, and allowed to sit 5 min before removal of the solvent. Dehydrated gel fragments were further dried under vacuum for 20 min. Gel fragments were first rehydrated with 7.5 μl of 20 ng/μl trypsin solution suspended in 25 mM ammonium bicarbonate, covered with an additional 7.5 μl of 25 mM ammonium bicarbonate, and digested at 37°C for 2 h. Peptides were recovered from the digests by adding 30 μl of acetonitrile/aqueous 25 mM ammonium bicarbonate (50:50, v/v) and vortexing for 10 min, and transferring the liquid phase to a new tube. This step was then repeated, with a quick vortexing, and samples were pooled and lyophilized to dryness.

Lyophilized peptide samples were resuspended in 30 μl of 10% acetonitrile/0.1% acetic acid/0.01% trifluoroacetic acid (v/v), pH 2.5. Five microliters of the resuspended sample was injected for each liquid chromatography MS analysis. The chromatography system used was a dual syringe pump (140B; Applied Biosystems, Foster City, CA) operated at 50 μl/min. The solvent flow was split 1:25 in a stainless steel Valco T to deliver 2 μl/min through a 30-cm fused silica capillary (150 μm i.d./360 μm o.d.) packed with Jupiter 5-μm C18 (Phenomenex, Torrence, CA). The column was packed in a stainless steel union with a 1/16-in. o.d. stainless steel frit (Upchurch Scientific, Oak Harbor, WA). The union was also used as the contact point to apply the electrospray source potential. The effluent from the column was directed into the ion source with a 15-cm-long (75 μm i.d./185 μm o.d.) hand-pulled fused silica capillary. The solvents used for chromatography were A [0.1% acetic acid/0.01% trifluoroacetic acid (v/v)] and B [60% acetonitrile/0.1% acetic acid/0.01% trifluoroacetic acid (v/v)]. A 60-min gradient from 10 to 95% solvent B was used to elute peptides off the column. The quadrupole iontrap mass spectrometry was performed on an LCQ (Thermo Finnigan, San Jose, CA) with ring electrode and skimmer potentials of +40 and +34 V, respectively.

For peptide fingerprinting analysis, the mass spectra were collected in a data-dependent manner in centroid mode over a range from 400 to 2000 m/z. Selection for a higher resolution "zoomscan" analysis was done using an 8 m/z isolation window on the most abundant peak observed in the first stage of MS. This LCQ function provided a higher resolution m/z measurement over a 10 m/z window and allowed for the direct charge state determination for peptides with a charge state up to 3+.

For MS/MS analysis, data were also collected in a data-dependent manner with the first stage of mass spectrometry collected in centroid mode over 400 to 2000 m/z with an ion inject time preset to 50 ms. Selection for the second stage of MS was done using an 8 m/z isolation window on the most abundant peak observed in the first stage of MS. A rise time of 50 ms, activation Q setting of 0.250, and 40% relative collision energy were used to dissociate the ions.

For protein fingerprinting analyses, peptide masses obtained from an MS analysis were entered into ProFound (http://prowl.rockefeller.edu/cgi-bin/ProFound), a program that fits the peptide masses measured by MS with predicted tryptic fragments of each protein in a large database (Zhang and Chait, 2000). ProFound calculates a probability value for each aligned protein such that the sum of all the matched probabilities is 1. As such, if only one protein fits the data well then a probability that is close or equal to 1 will be assigned. In cases where several proteins fit the data well, the sum of the probabilities for proteins with a good fit will approach 1. For the ProFound alignments, we used the National Center for Biotechnology Information nonredundant rodent database and a mass accuracy of 200 ppm. No restrictions were put on the potential protein masses to be used for alignment.

In some cases, identification of proteins by peptide fingerprinting was confirmed by MS/MS analysis, a procedure that provides sequence information on individual peptides. For the MS/MS results, MS-Tag (http://prospector.ucsf.edu/ucsfhtml3.4/mstagfd.htm) was used to search the current National Center for Biotechnology Information database of rat proteins. The product ion MS/MS spectra for each parent peptide were summed and a list of m/z and intensity was generated for all product ions. Ions detected at >10% relative abundance were entered along with the monoisotopic mass for the parent ion. The database was searched for peptide matches using a 200-ppm parent and 1500-product ion m/z window with an allowance for up to two missed trypsin cleavage sites.

Immunoprecipitation of CYP3A. The polyclonal antibody against rat CYP3A was conjugated to Ultralink beads according to the manufacturer's instructions (Pierce Chemical) and used for immunoprecipitation of CYP3A as follows. Microsomal samples from nicardipine-treated rats were incubated for 0 or 2 h as described above, except that the reaction was scaled up to 250 μl. The microsomal membranes and proteins were suspended in an equal volume of 2× immunoprecipitation buffer (final concentration was 0.9% NaCl, 0.1 M sodium phosphate, pH 7.4, 1% Nonidet P-40, 0.5% sodium deoxycholate, and 0.1% sodium dodecyl sulfate, 0.1 mg/ml phenylmethylsulfonyl fluoride, 0.07 mg/ml aprotinin, 1 mM orthovanadate). Samples were gently mixed at 4°C for 5 h. The beads were collected in Micro Bio-Spin columns, drained by gravity flow, and washed with 2 ml of immunoprecipitation buffer. CYP3A was gently eluted at room temperature by using 1 ml of 0.1 M glycine, 1% Nonidet P-40, and 1% CHAPS, pH 2.2, and immediately neutralized by adding 500 μl of 1 M Tris base, pH 7.4. Suspension of the beads in SDS-PAGE loading buffer and heating to 95°C for 5 min indicated that this elution procedure was sufficient to remove essentially all of the bound CYP3A. The eluant was transferred to a Centricon C-10 and concentrated to ~150 μl by centrifugation for 2000g for ~2.5 h. The equivalent of 15 μl of each concentrated sample was then analyzed by Western blot techniques as described above. In these analyses, the secondary antibody used for Western blot detection was raised in goat, the same host species as the antibody used for immunoprecipitation. This step combined with the gentle elution conditions, which eluted only trace amounts of the bound capture antibody from the column, eliminated any detectable interference by the capture antibody in the Western analyses.

Statistics. Statistical analysis of the density of the ubiquitin signal in Western blots was undertaken using a one-way analysis of variance followed by a Tukey's multiple comparison with SigmaStat 2.0 software (SPSS Science, Chicago, IL). A probability value of < 0.05 was used for both analyses.

Results

CYP3A and Ubiquitin-Conjugating Activity in Incubated Microsomes. We sought to develop a model system to study the molecular processes involved in the degradation of microsomal CYP3A proteins. Based on previous studies, we expected this system to require the addition of cytosolic proteins to the microsomal samples. Therefore, we undertook initial studies to characterize the loss of CYP3A protein in microsomes incubated in the presence or absence of cytosol. These microsomes were obtained from the livers of rats treated for 7 d with 100 mg/kg/day nicardipine, a calcium channel antagonist that is also an efficacious CYP3A inducer (Zangar et al., 1999). Western blot analyses with specific anti-peptide antibodies for CYP3A23 and CYP3A2 indicated the formation of HMM bands in the incubated microsomes (Fig. 1A). Although these HMM bands were characteristic of ubiquitinated proteins, we knew of no reports demonstrating ubiquitination of ER proteins in the absence of cytosol and therefore proceeded to more extensively characterize the formation of the HMM protein conjugates. To determine whether formation of these HMM bands was specific for

proteins that are ubiquitinated, we also probed these blots for CYP2E1, which is known to be ubiquitinated, and CYP4A, which is not known to be ubiquitinated. CYP2E1 formed HMM bands in the incubated microsomes, although the amount of HMM CYP2E1 formed relative to the intact CYP2E1 protein was much less than observed for the CYP3A proteins (Fig. 1A). In contrast to CYP3A and CYP2E1, no HMM banding of CYP4A was observed in the incubated microsomes (Fig. 1A), suggesting that the conjugating reaction was selective for certain P450s. The addition of cytosol to these samples resulted in the loss of the HMM CYP3A23, CYP3A2, and CYP2E1 bands, consistent either with the degradation of HMM CYP3A by cytosolic proteases or with cytosol inhibiting the formation of the bands. (The ~80-kDa band detected with the CYP2E1 antibody in the lane containing cytosol is a cross-reactive cytosolic protein that is unaffected by incubation.)

To differentiate between cytosol-dependent degradation of the HMM CYP3A conjugates versus factors in cytosol that inhibit the formation of HMM CYP3A, we added varying amounts of cytosol to the microsomes either at the start of the 2-h incubation period or 1 h later. To eliminate interference of the cytosolic proteins with the Western blotting procedures, microsomes were recovered from the incubates by ultracentrifugation. Western analysis of microsomal pellets and cytosolic supernatants indicated that the majority (>90%) of the ~55-kDa and HMM CYP3A protein remained
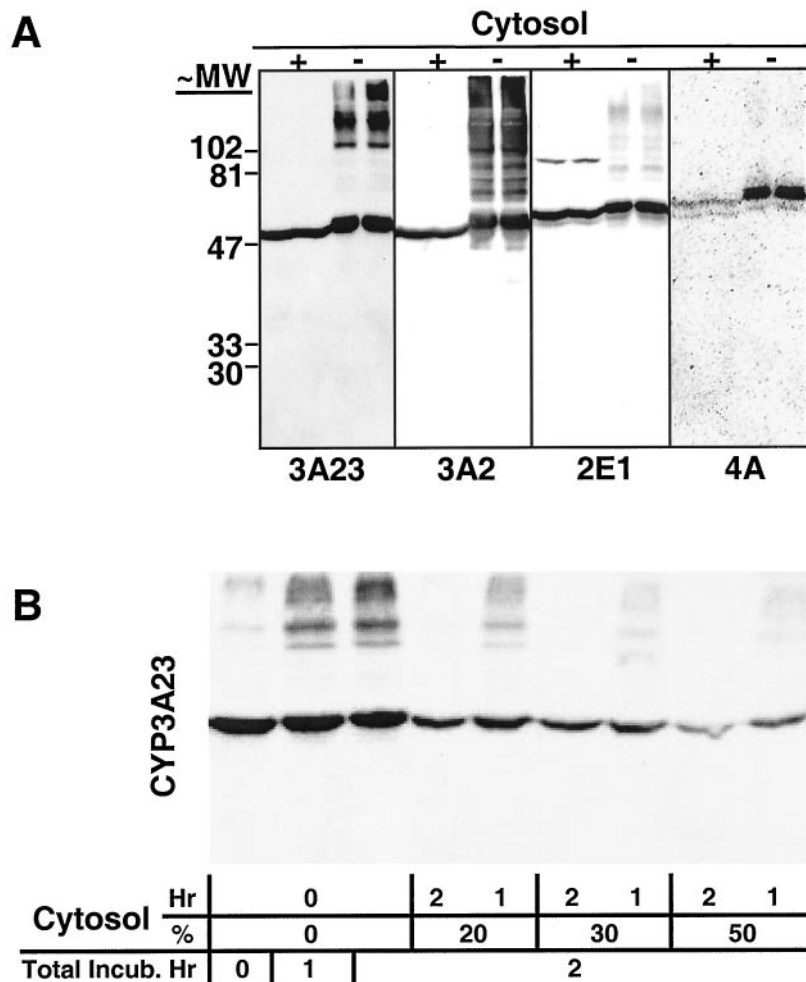

Fig. 1. Incubation of microsomes from nicardipine-treated rats results in the formation of high molecular mass bands (~MW) that are degraded in the presence of cytosol. A, microsomes were incubated for 2 h with or without cytosol. Samples were then fractionated using SDS-PAGE, transferred to nitrocellulose, and probed using antibodies specific for CYP3A23, CYP3A2, CYP2E1, or CYP4A. Approximate molecular mass, shown on the left, were taken from prestained standards on the CYP3A23 blot. Because all blots were run under similar conditions, protein migration on the other blots is similar but may vary slightly. B, microsomes were incubated at 37°C for 0, 1, or 2 h without cytosol or were incubated for 2 h with 20, 30, or 50% cytosol (v/v) added at the start of the incubation (2 Hr Cytosol) or 1 h later (1 Hr Cytosol). The protein concentration of 100% cytosol was 26 mg/ml. After incubation, microsomes were pelleted by ultracentrifugation and analyzed by Western blot procedures with a CYP3A23-specific antibody.

with the microsomal fraction (data not shown). A time-dependent increase in formation of the HMM CYP3A23 bands was observed in the microsomes incubated without cytosol after 1 and 2 h that was accompanied by a loss of the ~55-kDa CYP3A23 band (Fig. 1B). The addition of increasing amounts of cytosol during the second hour of incubation resulted in a loss of the HMM- and ~55-kDa CYP3A23 bands. This cytosol-dependent loss of the HMM CYP3A band was further increased when cytosol was added at the start of the incubation even though there was no additional loss of the ~55-kDa CYP3A23 band in the 20 and 30% cytosol samples. At 50% cytosol, the ~55-kDa band was decreased to a greater degree when cytosol was added at the start of the incubation rather than an hour later. Addition of protease inhibitors such as 20 μM lactacystin, 200 μM MG132, or 200 μM protease inhibitor I did not have any clear effect on the cytosol-mediated loss of HMM CYP3A bands (data not shown). In contrast, treatment of primary hepatocytes with the same concentrations of these reagents markedly increased immunodetectable levels of HMM ubiquitinated proteins (R. C. Zangar, et al., unpublished observations). Therefore, these results suggested that addition of cytosol resulted in the proteolytic loss of the HMM CYP3A23 bands that was not mediated by proteasomal degradation.

To better characterize the loss of ~55-kDa CYP3A23 protein and formation of the HMM CYP3A23 bands, microsomes were incubated in the absence of cytosol for 0 to 4 h. Again, formation of the HMM CYP3A23 bands was time-dependent and coincided with the loss of the ~55-kDa band (Fig. 2A). The HMM CYP3A bands migrated progressively upward with extended incubation times. This seemed to be a multistep process, in which the intact CYP3A first is converted to two bands of ~110 and 160 kDa (Fig. 2A, arrows) before being transferred to HMM bands of over 200 kDa. Densitometric analysis of the 55-kDa band indicated that the loss of this band was approximately linear for the first 3 h of the incubation period (Fig. 2B). To determine whether any detectable changes in the pool of total ubiquitinated proteins could be detected, a ubiquitin antibody capable of detecting all ubiquitinated proteins was used. In microsomes that were

not incubated, this antibody detected a smear of ubiquitinated proteins that was approximately 65 kDa or larger (Fig. 2C). These ubiquitinated proteins progressively migrated upward during the course of the incubation. Although the upward migration of CYP3A and the total pool of ubiquitinated proteins generally paralleled each other, at the early time points (i.e., 0.5 and 1 h), there is a marked increase in the very HMM ubiquitinated proteins, whereas very little HMM CYP3A is observed. This result suggested that the pool of HMM ubiquitinated proteins contained proteins other than CYP3A.

To better examine the loss of individual proteins with incubation, we used 2D gels that would allow us to examine protein spots that typically contained only one or two proteins rather than the multiple proteins typically present in one-dimensional SDS-PAGE protein bands. Visual examination of these silver-stained 2D blots revealed that very few proteins in this pI range were decreased with incubation (data not shown), supporting our other results that indicated the formation of the HMM proteins is a selective process. It should be noted that P450s typically have pI values of 8 to 9, a range traditionally very difficult to analyze by 2D gels, and we found that CYP3A and other basic proteins precipitated during IEF without forming distinct bands. For this reason, we did not use 2D gels to analyze basic proteins.

Detection of Ubiquitin in Immunoprecipitated HMM CYP3A. To determine whether ubiquitin is bound to the HMM CYP3A bands, we immunoprecipitated CYP3A and analyzed for ubiquitin by Western blot analysis. The HMM CYP3A immunoprecipitated with a decreased efficiency compared with the ~55-kDa CYP3A, presumably due to steric hindrance of antigenic sites in the HMM conjugates. Even so, sufficient HMM CYP3A was obtained for these analyses such that a clear increase in HMM CYP3A could be observed in a 2-h incubated sample compared with a control sample (Fig. 3). Probing of an identical blot with anti-ubiquitin showed that the HMM CYP3A band from the 2-h incubate had a marked increase in HMM ubiquitin conjugation. These data clearly demonstrated that CYP3A is complexed with ubiq-
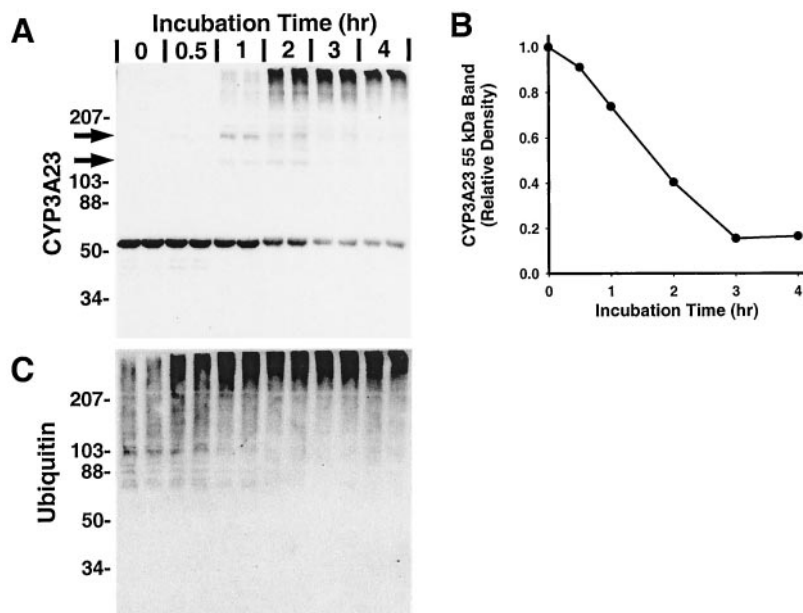

Fig. 2. Time-dependent changes in CYP3A23 and total ubiquitinated proteins in hepatic microsomes isolated from nicardipine-treated rats. Microsomes were incubated for 0 to 4 h at 37°C and then analyzed using Western blot techniques. A, Western blot analysis of CYP3A23. Each lane represents a separate microsomal incubation. B, graph of the time-dependent change in the density of the ~55-kDa CYP3A23 band in A. Each data point represents the average of two bands. C, Western blot analysis of total ubiquitinated proteins prepared using a polyclonal ubiquitin-specific antibody.

uitin in these microsomal samples without the addition of cytosol.

Formation of HMM Conjugates Is Largely Insensitive to Conditions Designed to Elute Weakly Bound Membrane Proteins. Studies were undertaken to determine whether conditions known to free weakly bound proteins from lipid membranes would prevent formation of the HMM conjugates in the microsomal membranes. In these studies, microsomes were incubated with high salt buffer, low salt buffer, high pH buffer, or exposed to mild detergent before repelleting, resuspension, and analysis for CYP3A-conjugating activity. In all cases, the relative loss of the ~55-kDa CYP3A protein band was nearly the same as (at least 90% of) that observed with microsomes incubated in physiologically buffered solution, and formation of the HMM CYP3A and ubiquitin bands was similar between all samples (data not shown). These data indicate that any factors catalyzing the formation of HMM microsomal proteins were tightly bound to the membranes.

Formation of HMM Proteins in Microsomal Samples Is Distinct from Classical Ubiquitin Ligation System. To further investigate whether the HMM CYP3A banding was the result of a ubiquitination reaction, we examined the concentration-dependent interactions of ubiquitin and MeUb, a known inhibitor of ubiquitin ligation reactions. We were surprised to see that formation of the HMM CYP3A or ubiquitin bands was not dependent upon addition of ubiquitin. As shown in Fig. 4, there was little effect on the loss of the ~55-kDa CYP3A band or the formation of HMM CYP3A bands after addition of ubiquitin to the reaction mixture. The presence of low levels of ubiquitin (1 and 10 μM) in the reaction solution had only modest effects at best on the formation of the HMM ubiquitin bands, but the HMM ubiquitin bands did increase sharply at 100 μM ubiquitin. Because the K_d value for E1 binding with ubiquitin is in the submicromolar range, E1-mediated ubiquitination reactions would be expected to be nearly saturated by 10 μM ubiquitin (Haas and Siepmann, 1997). Therefore, the increase in protein ubiquitination at 100 μM ubiquitin is unlikely to be mediated by E1 ubiquitin-activating enzyme.

MeUb inhibited both the formation of the HMM CYP3A and the loss of the ~55-kDa CYP3A23 band in a concentration-dependent manner. Even so, inhibition of this reaction
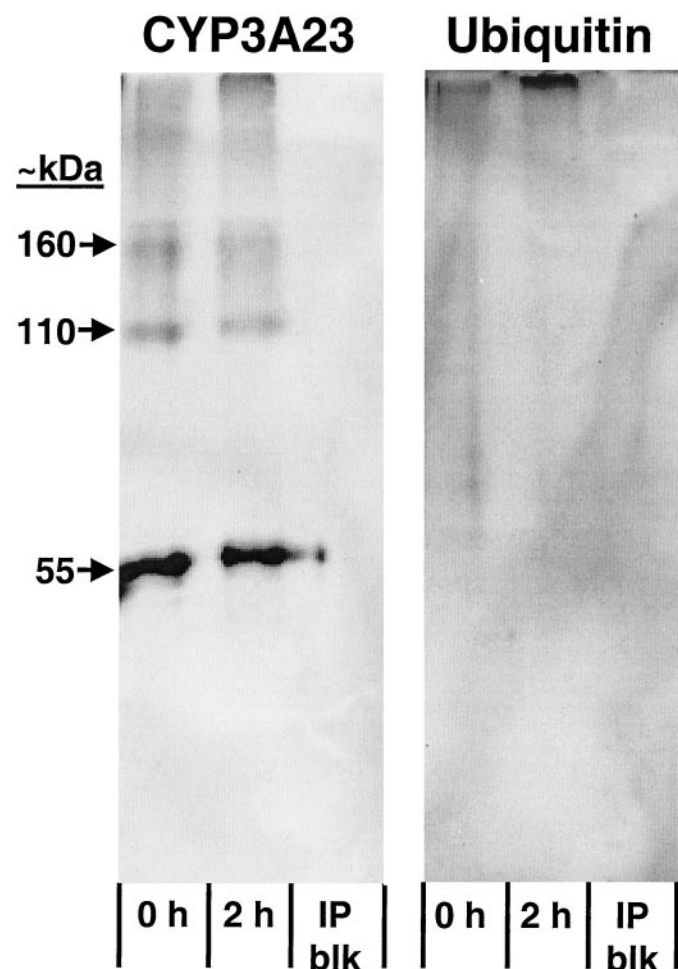

Fig. 3. Presence of HMM ubiquitin in CYP3A immunoprecipitates. CYP3A was immunoprecipitated as described under *Experimental Procedures*. Samples were then analyzed using Western blot procedures and CYP3A23-specific polyclonal and ubiquitin-specific monoclonal antibodies. Approximate mass of CYP3A23 bands is indicated by arrows.
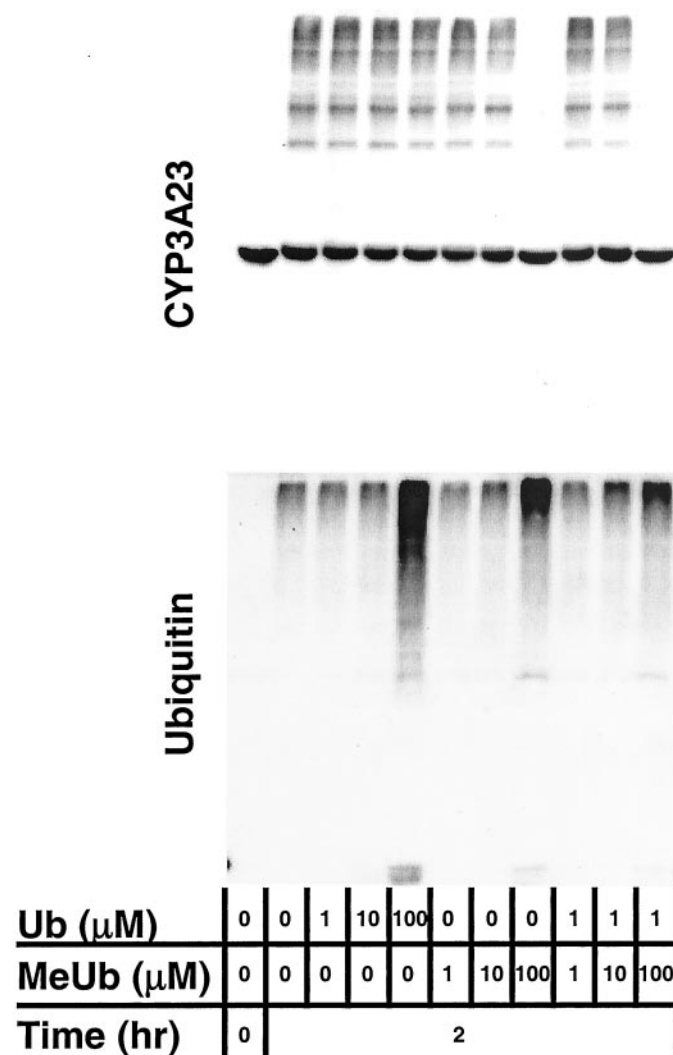

Ub (μM)	0	0	1	10	100	0	0	0	1	1	1
MeUb (μM)	0	0	0	0	0	1	10	100	1	10	100
Time (hr)	0	2									

Fig. 4. Concentration-dependent effects of ubiquitin and MeUb on the formation of HMM CYP3A23 or ubiquitin proteins. Microsomes were incubated for 2 h at 37°C in the presence of 0, 1, 10, or 100 μM added ubiquitin and/or MeUb. Samples were then analyzed by Western blot with polyclonal antibodies specific for CYP3A23 or ubiquitin.

did not yield the mono- or di-ubiquitinated CYP3A bands that would be expected of MeUb inhibition of polyubiquitination. In contrast to its inhibitory effects on the formation of HMM CYP3A, MeUb not only did not block the formation of HMM ubiquitin proteins but also actually seemed to stimulate this reaction at high concentrations (Fig. 4), indicating that the formation of the HMM ubiquitin was atypical of classical ubiquitin ligase reactions. The fact that MeUb had opposing effects on the formation of HMM CYP3A and HMM ubiquitin demonstrated that these two processes could be separated experimentally. We should note that the polyclonal ubiquitin antibody used in these studies seemed to be less sensitive for MeUb than ubiquitin, so that the decreased HMM ubiquitin signal detected in the 100 μM MeUb lanes relative to the 100 μM regular ubiquitin lanes is not necessarily indicative of lower levels of HMM MeUb. We have also examined the effects of K48R ubiquitin, which would specifically block ubiquitination on a lysine commonly used in polyubiquitin conjugation. Similar to the results obtained with regular ubiquitin, we found addition of this ubiquitin analog had little if any effect on the formation of HMM CYP3A conjugates, but that at 100 μM K48R there was an increase in the amount of HMM ubiquitin proteins (data not shown).

It is also important to realize that typically "ubiquitin" antibodies, including the ones used herein, preferentially recognized polyubiquitin over monoubiquitin. Because ubiquitin is an essential cellular molecule that is highly conserved between species (Wilkinson, 1995), binding of antibodies to monoubiquitin may be lethal to the antibody-producing cell. As such, analysis of stained gels indicated that very little (<10%) of the added ubiquitin was converted to HMM bands in the 100 μM ubiquitin sample. Therefore, the greater band intensity in HMM bands rather than the 8-kDa monoubiquitin band (at the very bottom of the blot) observed in the ubiquitin Western blot (Fig. 4) is not indicative of an efficient conversion of monoubiquitin to polyubiquitin in these samples, although these results do clearly indicate an increase in the levels of HMM polyubiquitin in the incubated samples.

To further examine the role of ubiquitin ligation in the formation of HMM CYP3A, reactions were tested in the absence of ATP and Mg^{2+}, which are essential cofactors for ubiquitin-activating enzyme E1. In some cases, apyrase was also added to remove any trace amount of ATP that might be present in the microsomal fractions. These studies indicated that the presence or absence of 5 mM ATP and/or Mg^{2+} had only a modest effect on the loss of the ~55-kDa CYP3A. That is, in the absence of added ATP in the reaction mixture, there was less than a 30% decrease in the formation of HMM CYP3A bands or loss of the ~55-kDa CYP3A band and that the addition of 0.1 unit/μl of apyrase had no further effect than observed with ATP removal alone (data not shown). Not adding Mg^{2+} had no clear effect on the conjugation reactions and the addition of 5 mM EDTA to incubated microsomes that lacked added Mg^{2+} did not seem to alter the formation of the HMM CYP3A bands. We also compared levels of E1 protein in microsomes and cytosol using Western blotting procedures. Although readily detectable levels of E1 protein were present in hepatic cytosol from rats treated with nicardipine, levels in microsomal fractions were extremely low by comparison (Fig. 5). Therefore, the formation of HMM CYP3A or ubiquitin conjugates in the incubated microsomes

does not require the presence of ATP, cytosol, or Mg^{2+} and is unlikely to be dependent on ubiquitin-activating enzyme E1 activity.

Protein Fingerprinting Analysis of HMM Protein Bands. Although monoubiquitin is normally a cytosolic protein, Western analysis showed a pool of polyubiquitinated protein in the microsomes before incubation that did not seem to be associated with CYP3A (Fig. 2C, 0-h incubates). Conceivably, de-ubiquitinating enzymes could release ubiquitin from these microsomal proteins and provide free ubiquitin that could conjugate to microsomal CYP3A even in the absence of added ubiquitin. Much of the HMM CYP3A migrated above 200 kDa, indicating that if ubiquitin conjugation alone accounted for the increase in CYP3A mass, there must be a molar ratio of over 15 ubiquitin molecules per each CYP3A molecule. Trypsin digestion and tandem mass spectrometry can be used to confirm the presence of ubiquitin in conjugated proteins (W. Li, personnel communication). Therefore, to determine whether levels of ubiquitin in the HMM bands were sufficient to account for the upward migration of CYP3A, we identified the most abundant proteins present in the HMM bands using in-gel trypsin digestion and MS analysis. Due to competition between peptides for ioniza-
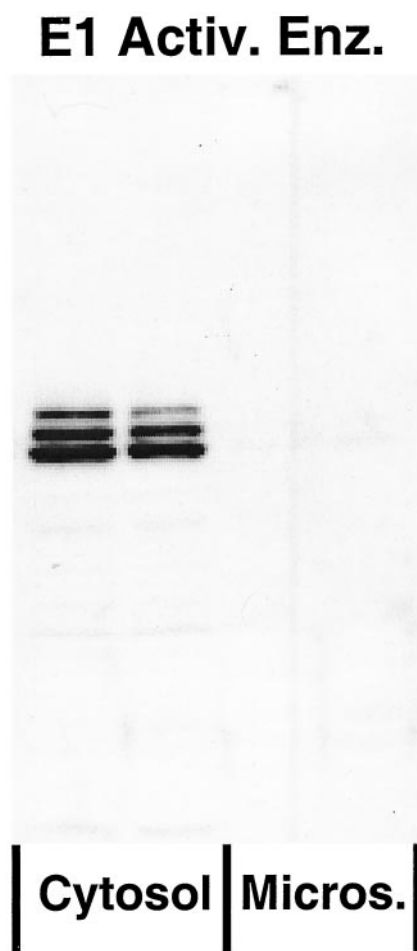

Fig. 5. Levels of E1 ubiquitin-activating enzyme are very low in microsomes compared with cytosol. Hepatic cytosol and microsome samples from rats treated with 100 mg of nicardipine/kg/day for 1 week were analyzed by Western blot with an antibody specific for E1 ubiquitin-activating enzyme.

tion energy within the MS, peptides derived from low-abundance proteins may be detected less frequently or not at all.

No ubiquitin was added to the microsome samples used for these initial MS analyses. We analyzed the section of the gel containing the ~55-kDa band associated with the CYP3A protein. Before incubation of microsomes from nicardipine-treated animals, only CYP3A2 and CYP3A1/23 were identified in the ~55-kDa band (Table 1). Combined, the probability for these CYP3A proteins was ~1.0. Alignment with the next most abundant non-CYP3A protein was the mouse NK-tumor recognition protein (163 kDa), which gave a probability of 1.1×10^{-11}. After incubation, only microsomal epoxide hydrolase, a 53-kDa protein, was identified in the corresponding region of the gel. Of the 10 peptides masses derived from epoxide hydrolase that were identified in the postincubation sample, only three were detected in the preincubation sample, suggesting that competition from the more abundant CYP3A-derived peptides prevented MS detection of some epoxide hydrolase peptides in the preincubation sample. Three peptides from a single protein are typically not sufficient for that protein to be identified by the peptide fingerprinting techniques used herein.

We also analyzed the HMM proteins present in the top 2 mm of the gel by using the MS fingerprinting techniques. In the preincubation microsome sample, the only peptides identified in the HMM region were associated with trypsin autolysis. Analysis of the HMM proteins in postincubation microsomes identified CYP3A1/23 and CYP3A2 but not any other proteins (Table 1). The combined probability of the CYP3A alignments was ~1.0, whereas alignment with the next most abundant protein, mouse myosin VIIa (288 kDa), gave a probability of 3.8×10^{-9}. The presence of the CYP3A proteins in the HMM portion of the gel was also confirmed by MS/MS sequence analysis of eight peptides (Table 1). In extracts from an in-gel digestion undertaken at the same time as the digests described above but prepared with 100 μM ubiquitin, we could readily detect peptides from monoubiquitin (~8-kDa band) that accounted for 67% of the intact ubiquitin sequence (Table 1). Letting the MS automatically select peptides for MS/MS, a procedure that selects the most abundant peptide in each spectra for MS/MS analysis and was used above to identify the eight CYP3A peptides, did not yield a single peptide that corresponded to the ubiquitin analysis. Directing the MS to specifically search and perform MS/MS analysis on peptides with masses corresponding to those observed in the monoubiquitin analysis did detect one ubiquitin peptide in the HMM band in samples incubated with 100 μM ubiquitin. These results strongly suggest that in the HMM region of the microsomes incubated without added ubiquitin, ubiquitin conjugates were at much lower levels than the CYP3A proteins. Therefore, these data suggest the formation of the HMM CYP3A conjugates was unlikely to result primarily from classical polyubiquitination, a process that would yield a large molar excess of ubiquitin (in the form of conjugates) relative to CYP3A.

Substrate-Mediated Stabilization of CYP3A Protein in Incubated Microsomes. To determine whether CYP3A protein conjugation observed in microsomes from nicardipine-treated rats might be related to the molecular processes that stabilize CYP3A protein in living cells, we treated microsomes with agents previously shown to stabilize CYP3A protein in vivo and in primary cultured hepatocytes (Eliasson et al., 1994). These CYP3A substrates, clotrimazole, ketoconazole, and erythromycin, prevented the loss of the ~55-kDa CYP3A23 band and the formation of the HMM CYP3A23 bands (Fig. 6). In contrast to this effect, none of these CYP3A substrates decreased the upward migration of the pool of proteins detected using the ubiquitin antibody. These results suggested that CYP3A substrates acted directly on CYP3A rather than any potential conjugating enzymes and supported the hypothesis that substrate-mediated stabilization results from altered CYP3A conformation. These results also confirmed that the amount of HMM ubiquitin conjugates formed was independent of HMM CYP3A levels.

To determine whether CYP3A substrate would also prevent the loss of the ~55-kDa CYP3A band previously observed in the presence of cytosol (Fig. 1B), we incubated microsomes with 20% cytosol and 10 μM clotrimazole. In addition to blocking the formation of the HMM CYP3A bands, the addition of clotrimazole also completely blocked the loss of the ~55-kDa CYP3A23 band. That is, in the presence clotrimazole and cytosol, CYP3A23 band density was $101 \pm 5\%$ (mean $\pm$ S.E., $n = 3$) of levels in microsomes that had not been incubated. These results indicate that inhibition of the formation of the HMM CYP3A bands by substrate also prevented the cytosol-mediated degradation of this protein.

Nicardipine is also a CYP3A substrate and therefore could potentially stabilize this protein. To examine this possibility, we treated the incubated microsomes with 0, 10, 30, 100, 300,

TABLE 1
Protein fingerprinting results obtained from the mass spectrometric analysis of tryptic peptides and protein alignment using ProFound

The ~55 kDa band and the HMM bands were determined in samples without added ubiquitin. The ubiquitin band was analyzed in a separate sample that contained 100 μM ubiquitin. Probability values for multiple hits on the same or very closely related gene product were summed. For example, in the case of the ~55-kDa band, ProFound identified two separate entries for CYP3A2 and assigned each a probability of 0.31. The last column identifies the number of peptides for which sequence information was obtained by MS/MS analysis that confirmed that the peptide was from the indicated CYP3A protein. CYP3A1 and CYP3A23 are 98.6% identical. As such, we were typically unable to distinguish peptides from these two proteins using this analysis.

Gel Section	Incub.	Protein Identified	Peptides Aligned	Coverage	Probability	MS/MS Peptides
	h			%		
~55-kDa band	0	CYP3A2	16	33	0.62	
		CYP3A1/23	16	39	0.38	
	2	μS Epoxide Hydrolase	10	29	1.0	
HMM Bands	0	none				
	2	CYP3A1/23	13	43	0.99	5
		CYP3A2	10	34	0.000004	3
Ubiquitin (8 kDa)	0	Ubiquitin	7	67	1.0	

or 1000 μM nicardipine to determine effects on CYP3A HMM band formation. Ten micromolar nicardipine partially blocked the CYP3A23 HMM band formation and concentrations of 100 μM or greater seemed to completely block this reaction (Fig. 7A). We also determined whether nicardipine stabilized CYP3A23 protein in primary cultured rat hepatocytes in which CYP3A23 levels were previously induced with phenobarbital or dexamethasone. After 24-h induction with these drugs, cells were cotreated with cycloheximide (to block protein synthesis) and nicardipine or DMSO. DMSO is a potent stabilizing agent of CYP3A protein in primary cultured hepatocytes (Zangar and Novak, 1998) and was used as a positive control in this study. These studies showed that addition of nicardipine prevented the degradation loss of CYP3A23 protein to a degree similar to that observed with DMSO (Fig. 7B).

Formation of HMM Protein Conjugates Is Dependent upon Extended in Vivo Treatment with Agents That Transcriptionally Induce and Stabilize CYP3A. To determine whether the microsomal CYP3A-conjugating activity was dependent upon nicardipine treatment, we examined hepatic microsomes from rats treated with 0, 25, 50, or 100 mg nicardipine/kg/day for 7 days. CYP3A2 was measured in this study because, unlike CYP3A23, CYP3A2 can be readily detected in untreated rats. Microsomes from rats treated with either 50 or 100 mg of nicardipine/kg/day formed HMM CYP3A2 conjugates, although greater activity was observed in microsomes from the animals that received the higher dose (Fig. 8). In contrast, in microsomes from control rats or those treated with 25 mg nicardipine/kg/day, no upward shift in CYP3A2 was observed. Similarly, the

incubation-dependent upward migration of the pool of ubiquitinated proteins was only observed at the two higher doses. These results indicated that the presence of the CYP3A protein conjugation reaction in the microsomal fractions was dependent upon in vivo treatment with nicardipine at doses of 50 mg/kg/day or higher and correlated with the ubiquitin conjugation reaction.

Analysis of the intensity of the signal detected with the anti-ubiquitin antibody in samples that were not incubated (0-h samples; Fig. 8, bottom) was also undertaken. A trend toward decreasing signal with increasing nicardipine dose was observed, such that relative levels of 100 ± 22, 67 ± 15, 48 ± 1, or 35 ± 7 (mean $\pm$ S.E.) were observed for the treatments of 0, 25, 50, or 100 mg/kg/day. The 100-mg/kg/day dose resulted in a statistically significant decrease in ubiquitin signal relative to the samples from untreated animals. These results suggest that although nicardipine treatment induced the microsomal conjugation reaction, this treatment did not increase levels of ubiquitinated proteins in the microsomal fraction.

To further characterize the nicardipine-dependent induction of CYP3A-conjugating activity, we treated rats by gavage with 100 mg of nicardipine/kg/day for 1, 2, or 3 days. We have observed with some drugs (although typically not with nicardipine) that the rats will occasionally decrease food intake on the 1st day of dietary treatment. Although no changes in weight gain (or other overt signs of toxicity) are observed with extended treatment of animals with nicardi-
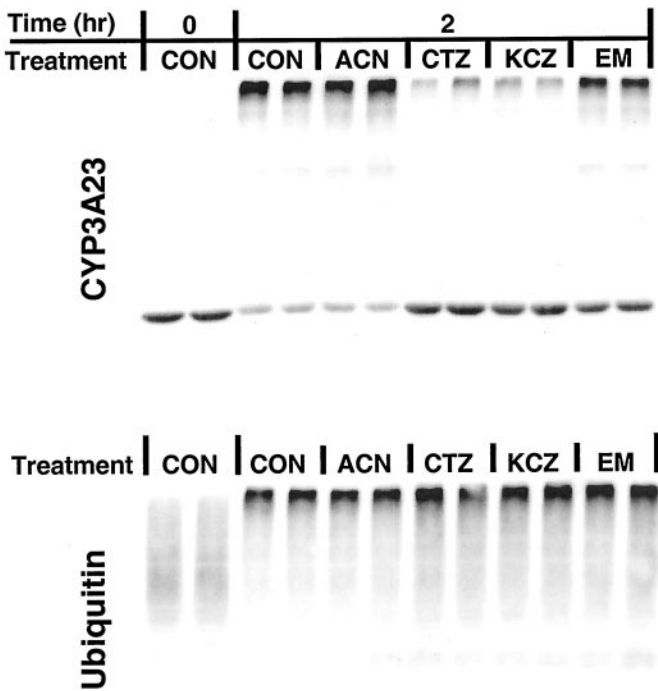

Fig. 6. Substrate-mediated inhibition of the formation of HMM CYP3A23. Microsomes from rats treated with 100 mg of nicardipine/kg/day were incubated at 37°C for 2 h in the absence (CON) or presence of 0.1% acetonitrile (ACN; vehicle for CYP3A substrates), 10 μM clotrimazole (CTZ), 10 μM ketoconazole (KCZ), or 100 μM erythromycin (EM). Western blot analyses with polyclonal antibodies specific for CYP3A23 (A) or ubiquitinated (B) protein levels are shown.
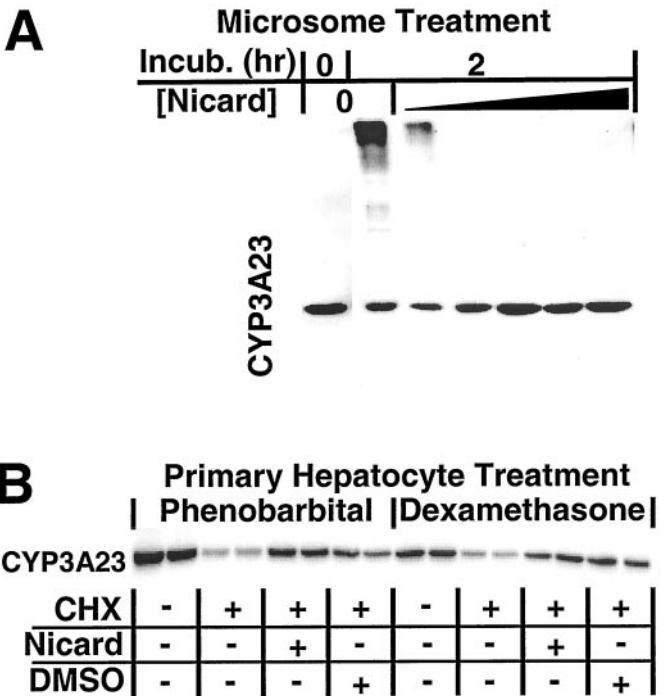

Fig. 7. Nicardipine stabilizes CYP3A protein in incubated microsomes and primary cultured rat hepatocytes. A, microsomes from rats treated with 100 mg of nicardipine/kg/day were incubated at 37°C for 2 h in the presence of 0.9% acetonitrile alone or in combination with 10, 30, 100, 300, or 1000 μM nicardipine and then analyzed using Western blot procedures and a specific CYP3A23 antibody. B, primary rat hepatocytes were cultured for 72 h, treated with phenobarbital, and dexamethasone for 24 h to induce CYP3A levels, and then cotreated with 10 μM cycloheximide (CHX) alone or with 330 μM nicardipine or 0.1% DMSO for 6 h. Cells were then harvested, and microsomes prepared and analyzed for CYP3A23 levels with Western blot procedures.

pine, the treatment of animals by gavage avoided any potential delay in initiation of the dosing regimen. We observed that nicardipine-mediated induction of CYP3A23 could be detected within 24 h after the first treatment and increased progressively until day 3 (Fig. 9). In contrast, the formation of HMM CYP3A protein bands was only detected in one sample from a rat treated for 3 days. Similarly, only this one sample demonstrated an upward shift in the pool of ubiquitinated proteins when analyzed with the ubiquitin antibody (data not shown). These data indicated that induction of CYP3A preceded induction of the microsomal protein-conjugating activity by several days.

To examine whether nicardipine's induction of the microsomal protein-conjugating activity was associated with CYP3A induction or effects on calcium channels, we examined microsomes from rats treated with other drugs that have similar effects. Treatment of rats with dexamethasone, a prototypical CYP3A inducer, did not result in any loss of the ~55-kDa CYP3A23 band or formation of HMM CYP3A23 in isolated microsomes incubated for 2 h (Fig. 10A). We also examined microsomes isolated from rats treated for 2 weeks at 100 mg/kg/day with nifedipine, which like nicardipine is a dihydropyridine calcium channel antagonist, or diltiazem, a benzothiazinepine calcium channel antagonist. Microsomes from rats treated with either of these agents also did not exhibit any protein-conjugating activity (Fig. 10B). Overall, these results indicate that induction of the microsomal protein-conjugating activity is not closely associated with short-term CYP3A induction or the general effects of calcium channel antagonists.

It seems that nicardipine both transcriptionally induces CYP3A and stabilizes CYP3A protein. To investigate the possibility that extended treatment with other agents that increase CYP3A protein by both mechanisms might have similar effects on the formation of HMM CYP3A, we examined hepatic microsomes from rats treated with 50 mg/kg/day of clotrimazole or pregnenolone 16α-carbonitrile for 1 week. These samples did exhibit the formation of HMM CYP3A conjugates (Fig. 11). Therefore, it seems that formation of the HMM-CYP3A protein complexes in isolated microsomes is

dependent at least in part on extended induction of very high levels of CYP3A protein.

Discussion

We found that hepatic microsomes from nicardipine-treated rats catalyzed the formation of HMM protein conjugates. Although CYP3A2, CYP3A23, CYP2E1, and ubiquitin were substrates for this conjugation reaction, CYP4A and most other microsomal proteins were not. Proteolysis was minimal in the isolated microsomes because there was no detectable loss of the ~55-kDa CYP3A protein in incubated microsomes that lacked the protein-conjugating activities (i.e., microsomes from rats not treated with high doses of nicardipine) and the HMM CYP3A proteins were maintained out to 4 h of incubation (Fig. 2). Attempts to strip the protein-conjugating activity by using various buffer systems known to remove weakly bound proteins from lipid membranes were unsuccessful, indicating that any factors associated with this conjugating activity were tightly bound to the ER membrane and were not cytosolic contaminants. Immunoprecipitation studies with CYP3A demonstrated that the HMM CYP3A was conjugated to ubiquitin. However, because the reaction was not dependent on addition of ATP, Mg^{2+}, or cytosol to the microsomes, this reaction seemed to be mechanistically distinct from the classical model of ubiquitin ligation. MS fingerprinting analysis of the HMM region of the gel also strongly suggested that CYP3A proteins were in molar excess to ubiquitin, a relationship opposite what would be expected if the HMM CYP3A bands were primarily due to polyubiquitination. It is possible that there is ubiquitin conjugated to microsomal E2 enzymes that could be transferred to CYP3A. Still, each E2 protein can bind only a single ubiquitin and, in the absence of E1 and ATP, this activated form of ubiquitin cannot be replenished. CYP3A protein is at very high levels in microsomes from nicardipine-treated rats, such that the darkest protein band observed in stained gels comigrated with the CYP3A protein and this band was primarily shifted to HMM proteins after incubation. Polyubiquitinated proteins are in low abundance in microsomes relative to cytosol
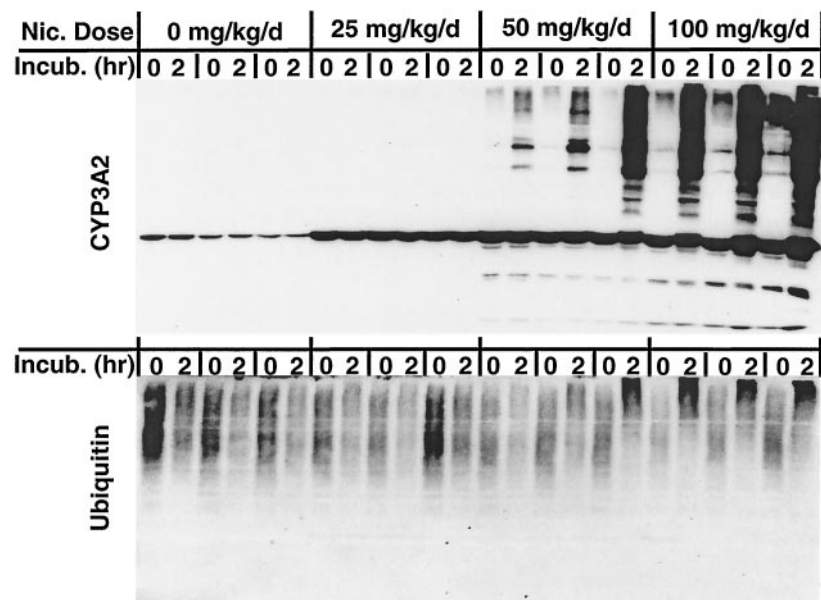

Fig. 8. Dose-dependent effects of nicardipine on the formation of HMM CYP3A2 or ubiquitinated proteins. Rats were treated with 0, 25, 50, or 100 mg of nicardipine/kg/day for 1 week and hepatic microsomes were isolated. Microsomes were incubated for 0 or 2 h at 37°C and then analyzed with Western blot techniques that used polyclonal antibodies specific for CYP3A23 or ubiquitin. The results of three different rats per treatment are shown such that each 0- and 2-h pair of samples represents microsomes taken from an individual animal.

(R. C. Zangar and A. L. Kimzey, unpublished observations) and in vivo nicardipine treatment decreased this limited pool of ubiquitinated microsomal proteins to ~35% of control levels. Therefore, it seems implausible that these microsomes contain enough ubiquitin, a cytosolic protein, in either free or bound forms to convert the majority of an abundant protein such as CYP3A into HMM protein conjugates by a classical ubiquitination reaction.

Overall, the data presented herein support a model in which protein conjugation in the microsomes can occur independent of additional polyubiquitination. Because addition of monoubiquitin to the incubation reaction was not required for the upward migration of the pool of ubiquitin proteins (Fig. 4, first two lanes), this upward migration was most probably due to ubiquitinated proteins forming larger complexes by conjugation to themselves or to other proteins in the microsomes rather than further polyubiquitination. Because the antibodies used in this study preferentially detected ubiquitin-protein conjugates over monoubiquitin, the

increased signal intensity in incubated microsomes detected by the ubiquitin antibodies most probably reflects an increase in protein-protein linkages involving ubiquitin rather than an increase in the total pool of ubiquitin. The cross-linking of polyubiquitin chains has been reported to be catalyzed by E2–25K, suggesting that a similar process could be occurring in the microsomes used in this study (Yao and Cohen, 2000).

It is interesting that the time course analysis of the CYP3A23 conjugation process indicated the early formation of two bands containing CYP3A23 that are approximately 2 and 3 times the mass of the intact protein (Fig. 2, arrows). In immunoprecipitated CYP3A samples, no increase in signal was detected in the Western blot for ubiquitin in the regions corresponding to these bands (Fig. 3), even though a chain of 13 ubiquitin molecules would be expected for each CYP3A molecule present for a mass shift of this magnitude. We analyzed the upper CYP3A band (i.e., the potential trimer) in the immunoprecipitated samples using trypsin digestion and
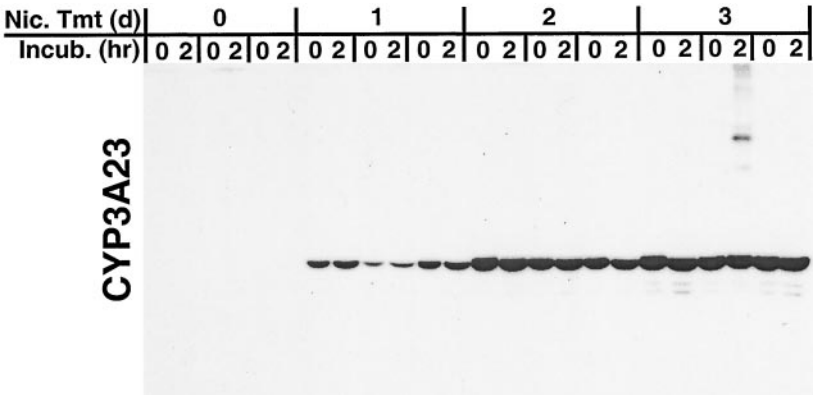

Fig. 9. Induction of CYP3A proceeds induction of protein-conjugating activity in rats exposed to nicardipine. Three rats per treatment were exposed to 100 mg of nicardipine/kg/day for 1 to 3 days. Hepatic microsomes were isolated and then incubated at 37°C for 2 h. Western blot analysis was used to compare the time dependence of the induction of the CYP3A23 protein and the microsomal ubiquitin-conjugating activities. The results of three different rats per treatment are shown such that each 0- and 2-h pair of samples represents microsomes taken from an individual animal.
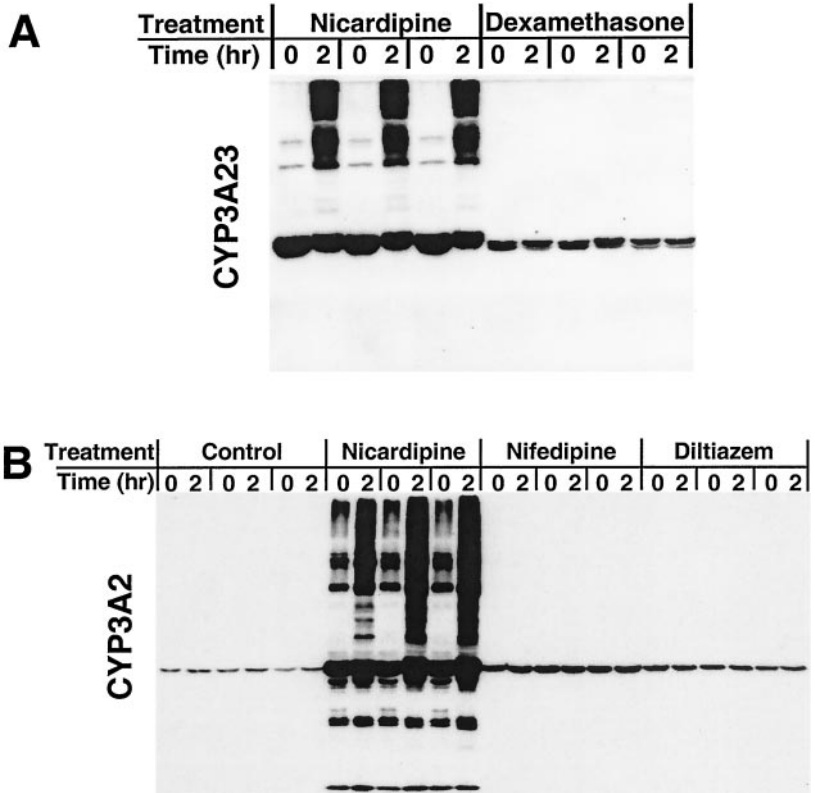

Fig. 10. Induction of microsomal CYP3A-conjugating activity is not characteristic of CYP3A inducers or calcium channel blockers. Hepatic microsomes from rats treated with a prototypical CYP3A inducer, dexamethasone (A), or with one of two calcium channel blockers, nifedipine and diltiazem (B), were compared with microsomes from nicardipine-treated rats. Three different rats per treatment were examined. Microsomes were incubated in the presence of ATP and ubiquitin at 37°C for 0 or 2 h. Western blot analysis was used to assess the presence of a microsomal CYP3A-conjugating activity with CYP3A23- or CYP3A2-specific antibodies.

tandem mass spectrometry but only peptides from CYP3A23 were detectable (data not shown). These results raise the possibility that CYP3A23 may form homocomplexes before conjugation with other proteins. Because MeUb inhibits formation of these potential oligomers, it seems likely that some interaction with ubiquitin is required before any CYP3A23 conjugates are formed. Therefore, it may be that the CYP3A23 in these bands is monoubiquitinated. In contrast, MeUb did not inhibit proteins already conjugated to ubiquitin from forming higher molecular mass complexes. This result suggests that once a protein is conjugated to ubiquitin, further ubiquitination is unnecessary for forming complexes of greater mass.

The HMM CYP3A protein complexes were degraded by cytosolic proteases in a process that was not affected by proteasomal inhibitors. The formation of ER protein complexes in living cells that contain ubiquitin but are refractory

Fig. 11. Sustained xenobiotic induction of CYP3A is sufficient to induce the microsomal conjugating activity. Rats were treated with 50 mg/kg/day of clotrimazole (CTZ) or pregnenolone 16α-carbonitrile for 1 week. Samples were then incubated for 2 h at 37°C, and analyzed for CYP3A levels by Western blot analysis as described under *Experimental Procedures*.

to cytosolic protein degradation has been reported previously (Johnston et al., 1998; Yokota et al., 2000). In a particularly relevant study, Yokoto et al. (2000) overexpressed urate oxidase that contained an altered N terminal, causing this enzyme to be retained in the ER. The urate oxidase formed lipoprotein complexes that immunostained positive for ubiquitin. Pulse-chase experiments readily detected degradation of the ubiquitin-urate oxidase complexes, but this degradation could not be attributed to proteasomal activity.

We demonstrated that CYP3A substrates prevented the loss of the ~55-kDa CYP3A band, the formation of HMM CYP3A bands, and the cytosol-mediated degradation of HMM CYP3A. This is the first evidence that CYP3A substrates may prevent the loss of CYP3A protein by decreasing conjugation and subsequent proteolysis. CYP3A substrates did not alter the formation of the HMM ubiquitin conjugates, consistent with the hypothesis that substrate binding alters CYP3A conformation and thereby stabilizes the protein, as suggested previously (Watkins et al., 1986). The inactivation and denaturation of CYP3A with agents such as 3,5-dicarbethoxy-2,6-dimethyl-4-ethyl-1,4-dihydropyridine, which destroys the central heme group, has been reported to accelerate the degradation of CYP3A by the ubiquitin/proteasome system (Korsmeyer et al., 1999). However, because CYP3A in the microsomes from nicardipine-treated rats was able to bind substrate in a manner that prevented subsequent conjugation, the nicardipine-induced CYP3A most probably contained a functional heme moiety that allowed substrate binding and associated conformational changes. This conclusion is consistent with our previous study that showed that in vivo nicardipine treatment increased CYP3A catalytic activity as well as CYP3A protein levels (Zangar et al., 1999). Therefore, it seems likely that in the absence of CYP3A substrate, even catalytically competent CYP3A is a substrate for this microsomal conjugation reaction. We also attempted to denature CYP3A by repeated freeze-thaw cycles, a process reported to increase microsomal CYP3A degradation by the 20S proteasome (Roberts, 1997). The repeated freeze-thaw cycles did not alter formation of the HMM CYP3A bands in microsomes from nicardipine-treated rats nor did it result in the formation of HMM CYP3A or ubiquitin conjugates in microsomes from nifedipine-, diltiazem-, dexamethasone-treated, or control rats (data not shown). These results further support that the microsomal-conjugating activity was dependent upon in vivo nicardipine treatment but was not dependent upon CYP3A denaturation.

Nicardipine doses of 50 and 100 mg/kg/day were required for induction of the microsomal ubiquitin ligase activity (Fig. 8). In contrast, nicardipine doses of between 5 and 15 mg/kg/day are sufficient for calcium receptor antagonism and antihypertensive effects in rats (Sorkin and Clissold, 1987). Furthermore, treatment with other calcium channel antagonists at comparably high doses for 2 weeks did not induce the microsomal ubiquitin ligase activity (Fig. 6B). Therefore, the mechanism by which nicardipine induced the microsomal conjugating activity seemed to be unrelated to calcium channel antagonism.

Nicardipine activates the pregnane X receptor (PXR) (Drocourt et al., 2001), which regulates CYP3A23 gene transcription and potentially could induce other proteins involved in a microsomal conjugating system. However, treatment of rats with dexamethasone, a prototypical CYP3A inducer that
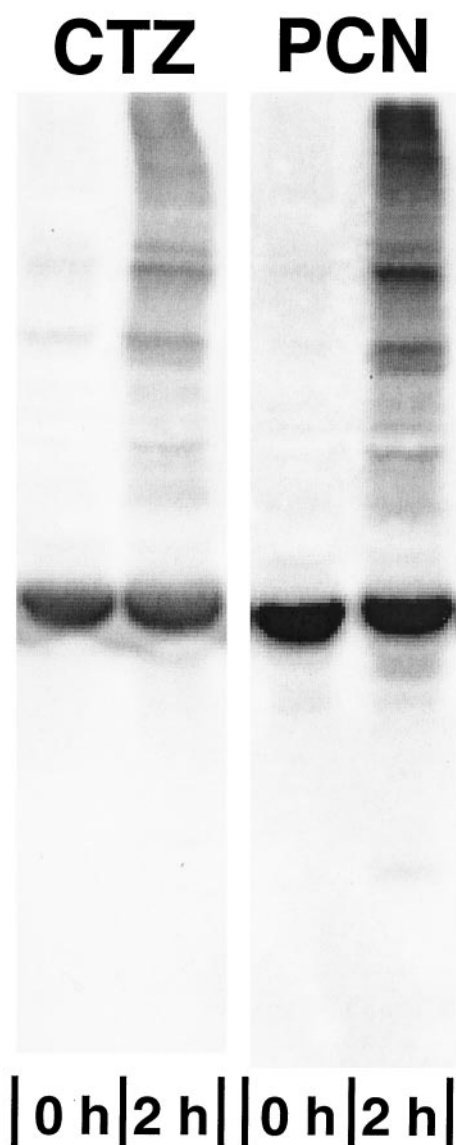
both induces and activates the PXR (Kliewer et al., 1998; Huss and Kasper, 2000), did not induce the formation of HMM CYP3A in incubated microsomes (Fig. 10A). Therefore, it seems that activation of PXR is not sufficient to induce the microsomal conjugating activity. Still, it is interesting that the short-term, direct effect of nicardipine on CYP3A in the incubated microsomes or primary cultured hepatocytes is to stabilize this protein (Fig. 7). This result suggests that the CYP3A conjugation reaction observed in microsomes from nicardipine-treated rats is not the result of direct interaction between nicardipine and CYP3A but is the result of sustained, high-level induction of CYP3A. This possibility was supported by studies that showed that microsomes from rats treated with the potent CYP3A-inducers clotrimazole and pregnenolone 16α-carbonitrile also exhibited the CYP3A conjugation reaction (Fig. 11). Therefore, it seems likely that extended maintenance of high levels of microsomal CYP3A is sufficient to induce or activate the conjugation process in microsomes. The loss of CYP3A protein under these circumstances is probably inhibited by the inducing agents, which are also CYP3A substrates.

Thus, taken together these data suggest that extended treatment with potent CYP3A inducers resulted in the induction or activation of microsomal factors that catalyzed the formation of both the HMM CYP3A and ubiquitin conjugates. Even so, this process was distinct from the classical ubiquitin/proteasome pathway. CYP3A substrates blocked this pathway, providing the first insight into the molecular processes involved into substrate-mediated stabilization of CYP3A.

References

Brodsky JL and McCracken AA (1999) ER protein quality control and proteasome-mediated protein degradation. *Semin Cell Dev Biol* **10:**507–513.

Correia MA, Davoll SH, Wrighton SA, and Thomas PE (1992) Degradation of rat liver cytochromes P450 3A after their inactivation by 3,5-dicarbethoxy-2,6-dimethyl-4-ethyl-1,4-dihydropyridine: characterization of the proteolytic system. *Arch Biochem Biophys* **297:**228–238.

Cosme J and Johnson EF (2000) Engineering microsomal cytochrome P450 2C5 to be a soluble, monomeric enzyme. Mutations that alter aggregation, phospholipid dependence of catalysis, and membrane binding. *J Biol Chem* **275:**2545–2553.

Debri K, Boobis AR, Davies DS, and Edwards RJ (1995) Distribution and induction of CYP3a1 and CYP3a2 in rat liver and extrahepatic tissues. *Biochem Pharmacol* **50:**2047–2056.

Drocourt L, Pascussi JM, Assenat E, Fabre JM, Maurel P, and Vilarem MJ (2001) Calcium channel modulators of the dihydropyridine family are human pregnane X receptor activators and inducers of CYP3A, CYP2B, and CYP2C in human hepatocytes. *Drug Metab Dispos* **29:**1325–1331.

Eliasson E, Mkrtchian S, Halpert JR, and Ingelman-Sundberg M (1994) Substrate-regulated, cAMP-dependent phosphorylation, denaturation, and degradation of glucocorticoid-inducible rat liver cytochrome P450 3A1. *J Biol Chem* **269:**18378–18383.

Guengerich FP (1999) Cytochrome P-450 3A4: regulation and role in drug metabolism. *Annu Rev Pharmacol Toxicol* **39:**1–17.

Haas AL and Siepmann TJ (1997) Pathways of ubiquitin conjugation. *FASEB J* **11:**1257–1268.

Hori H, Nembai T, Miyata Y, Hayashi T, Ueno K, and Koide T (1999) Isolation and characterization of two 20S proteasomes from the endoplasmic reticulum of rat liver microsomes. *J Biochem* **126:**722–730.

Huss JM and Kasper CB (2000) Two-stage glucocorticoid induction of CYP3A23 through both the glucocorticoid and pregnane X receptors. *Mol Pharmacol* **58:**48–57.

Johnston JA, Ward CL, and Kopito RR (1998) Aggresomes: a cellular response to misfolded proteins. *J Cell Biol* **143:**1883–1898.

Kliewer SA, Moore JT, Wade L, Staudinger JL, Watson MA, Jones SA, McKee DD, Oliver BB, Willson TM, Zetterstrom RH, et al. (1998) An orphan nuclear receptor activated by pregnanes defines a novel steroid signaling pathway. *Cell* **92:**73–82.

Koop DR and Tierney DJ (1990) Multiple mechanisms in the regulation of ethanol-inducible cytochrome P450IIE1. *Bioessays* **12:**429–435.

Korsmeyer KK, Davoll S, Figueiredo-Pereira ME, and Correia MA (1999) Proteolytic degradation of heme-modified hepatic cytochromes P450: a role for phosphorylation, ubiquitination, and the 26S proteasome? *Arch Biochem Biophys* **365:**31–44.

Lowry OH, Rosenbrough NJ, Farr AL, and Randall RJ (1951) Protein measurement for folin phenol reagent. *J Biol Chem* **193:**265–275.

Nelson DR, Koymans L, Kamataki T, Stegeman JJ, Feyereisen R, Waxman DJ, Waterman MR, Gotoh O, Coon MJ, Estabrook RW, et al. (1996) P450 superfamily: update on new sequences, gene mapping, accession numbers and nomenclature. *Pharmacogenetics* **6:**1–42.

Okita JR, Castle PJ, and Okita RT (1993) Characterization of cytochromes P450 in liver and kidney of rats treated with di-(2-ethylhexyl)phthalate. *J Biochem Toxicol* **8:**135–144.

Persson JO, Terelius Y, and Ingelman-Sundberg M (1990) Cytochrome P-450-dependent formation of reactive oxygen radicals: isozyme-specific inhibition of P-450-mediated reduction of oxygen and carbon tetrachloride. *Xenobiotica* **20:**887–900.

Ploegh HL (1997) Extraction of extrinsic proteins from membranes using sodium carbonate, in *Current Protocols in Protein Science* (Coligan JE, Dunn BM, Ploegh HL, Speicher DW and Wingfield PT eds) pp 4.2.42–4.2.43, John Wiley & Sons, New York.

Puntarulo S and Cederbaum AI (1998) Production of reactive oxygen species by microsomes enriched in specific human cytochrome P450 enzymes. *Free Radic Biol Med* **24:**1324–1330.

Roberts BJ (1997) Evidence of proteasome-mediated cytochrome P-450 degradation. *J Biol Chem* **272:**9771–9778.

Schwartz AL and Ciechanover A (1999) The ubiquitin-proteasome pathway and pathogenesis of human diseases. *Annu Rev Med* **50:**57–74.

Sherratt AJ, Banet DE, Linder MW, and Prough RA (1989) Potentiation of 3-methylcholanthrene induction of rat hepatic cytochrome P450IA1 by dexamethasone in vivo. *J Pharmacol Exp Ther* **249:**667–672.

Sorkin EM and Clissold SP (1987) Nicardipine. A review of its pharmacodynamic and pharmacokinetic properties, and therapeutic efficacy, in the treatment of angina pectoris, hypertension and related cardiovascular disorders. *Drugs* **33:**296–345.

Thummel KE and Wilkinson GR (1998) In vitro and in vivo drug interactions involving human CYP3A. *Annu Rev Pharmacol Toxicol* **38:**389–430.

Tierney DJ, Haas AL, and Koop DR (1992) Degradation of cytochrome P450 2E1: selective loss after labilization of the enzyme. *Arch Biochem Biophys* **293:**9–16.

von Wachenfeldt C, Richardson TH, Cosme J, and Johnson EF (1997) Microsomal P450 2C3 is expressed as a soluble dimer in *Escherichia coli* following modification of its N-terminus. *Arch Biochem Biophys* **339:**107–114.

Watkins PB, Bond JS and Guzelian PS (1987) Degradation of the hepatic cytochromes P-450, in *Mammalian Cytochromes P-450 II* (Guengerich FP ed) pp 173–192, CRC Press, Boca Raton, FL.

Watkins PB, Wrighton SA, Schuetz EG, Maurel P, and Guzelian PS (1986) Macrolide antibiotics inhibit the degradation of the glucocorticoid-responsive cytochrome P-450p in rat hepatocytes in vivo and in primary monolayer culture. *J Biol Chem* **261:**6264–6271.

Wilkinson KD (1995) Roles of ubiquitinylation in proteolysis and cellular regulation. *Annu Rev Nutr* **15:**161–189.

Yao T and Cohen RE (2000) Cyclization of polyubiquitin by the E2–25K ubiquitin conjugating enzyme. *J Biol Chem* **275:**36862–36868.

Yokota S, Kamijo K, and Oda T (2000) Aggregate formation and degradation of overexpressed wild-type and mutant urate oxidase proteins. Quality control of organelle-destined proteins by the endoplasmic reticulum. *Histochem Cell Biol* **114:**433–446.

Zangar RC and Novak RF (1998) Posttranslational elevation of cytochrome P450 3A levels and activity by dimethyl sulfoxide. *Arch Biochem Biophys* **353:**1–9.

Zangar RC, Okita JR, Kim H, Thomas PE, Anderson A, Edwards RJ, Springer DL, and Okita RT (1999) Effect of calcium channel antagonists nifedipine and nicardipine on rat cytochrome P-450 2B and 3A forms. *J Pharmacol Exp Ther* **290:**1436–1441.

Zangar RC, Springer DL, and Buhler DR (1993) Alterations in cytochrome P-450 levels in adult rats following neonatal exposure to xenobiotics. *J Toxicol Environ Health* **38:**43–55.

Zangar RC, Woodcroft KJ, Kocarek TA, and Novak RF (1995) Xenobiotic-enhanced expression of cytochrome P450 2E1 and 2B1/2B2 in primary cultured rat hepatocytes. *Drug Metab Dispos* **23:**681–687.

Zhang W and Chait BT (2000) ProFound, an expert system for protein Identification using mass spectrometric peptide mapping information. *Anal Chem* **72:**2482–2489.

Address correspondence to: Richard C. Zangar, Molecular Biosciences, Battelle PNNL, 902 Battelle Blvd., Richland, WA 99352. E-mail: richard.zangar@pnl.gov